

Research Article



## Enhanced *in Vitro* Anti-Tumor Activity of 5-Azacytidine by Entrapment into Solid Lipid Nanoparticles

Farhad Jahanfar<sup>1,2</sup>, Akbar Hasani<sup>2</sup>, Dariush Shanebandi<sup>3</sup>, Mohammad Rahmati<sup>2</sup>, Hamed Hamishehkar<sup>4\*</sup>

<sup>1</sup> Biotechnology Research Center and Student Research Committee, Tabriz University of Medical Sciences, Tabriz, Iran.

<sup>2</sup> Department of Biochemistry and Clinical Laboratories, Faculty of Medicine, Tabriz University of Medical Sciences, Tabriz, Iran.

<sup>3</sup> Immunology Research Center, Tabriz University of Medical Sciences, Tabriz, Iran.

<sup>4</sup> Drug Applied Research Center, Tabriz University of Medical Sciences, Tabriz, Iran.

### Article info

#### Article History:

Received: 12 February 2016

Revised: 25 April 2016

Accepted: 27 April 2016

ePublished: 25 September 2016

#### Keywords:

- 5-azacytidine
- Solid lipid nanoparticles
- SLN
- Cancer
- Cytotoxicity

### Abstract

**Purpose:** In this study the effectiveness of encapsulating of 5-azacytidine into the lipid nanoparticles was investigated and *in vitro* effect of encapsulated 5-azacytidine studied on MCF-7 cell lines

**Methods:** 5-azacytidine -loaded solid lipid nanoparticles were produced by double emulsification (w/o/w) method by using stearic acid as lipid matrix, soy lecithin and poloxamer 407 as surfactant and co-surfactant respectively. Particle size, zeta potential, surface morphology, entrapment efficiency and kinetic of drug release were studied. *In vitro* effect of 5-azacytidine on MCF-7 cell line studied by MTT assay, DAPI staining, Rhodamine B relative uptake, and also Real time RT-PCR was performed for studying difference effect of free and encapsulated drug on expression of RAR $\beta$ 2 gene.

**Results:** The formulation F5 with 55.84 $\pm$ 0.46 % of entrapment efficiency shows zero order kinetic of drug release and selected for *in vitro* studies; the cytotoxicity of free drug and encapsulated drug in 48 h of incubation have significant difference. DAPI staining shows morphology of apoptotic nucleus in both free and encapsulated drug, Rhodamine B labeled SLNs show time dependency and accumulation of SLNs in cytoplasm. Real time qRT-PCR doesn't show any significant difference ( $p > 0.05$ ) in expression of RAR $\beta$ 2 gene in both cells treated with free or encapsulated drug.

**Conclusion:** The results of the present study indicated that the entrapment of 5-azacytidine into SLNs enhanced its cytotoxicity performance and may pave a way for the future design of a desired dosage form for 5-azacytidine.

### Introduction

5-azacytidine was first synthesized in 1963<sup>1</sup> as an effective anti-cancer agent for the treatment of leukemia.<sup>2-4</sup> In 2004, the FDA approved the application of 5-azacytidine in treating myelodysplastic syndrome as the first drug effective in epigenetic therapy by inhibiting DNA methyltransferase.<sup>5</sup> Furthermore, 5-azacytidine inhibits protein production by being incorporated into RNA and interrupting its performance.<sup>6,7</sup> Although a few investigations have illustrated the effectiveness of experiments,<sup>8,9</sup> most clinical trials of the effects of 5-azacytidine on solid tumors are disappointing.<sup>10</sup> Due to its short half-life, 5-azacytidine is unable to permeate solid tumors and remain long enough to affect cancer cells.<sup>11</sup> The primary reason for this is the deactivation of 5-azacytidine by chemical hydrolysis or enzymatic deamination which results in short plasma stability.<sup>12,13</sup> A second reason is the need of particular variably expressed nucleoside transporters for cellular uptake.<sup>14</sup> There are two main strategies to overcome these obstacles. The first is to change the drug structure by chemical reactions like esterification.<sup>15</sup> Although this

strategy shows good results, the drug approving procedure for new drugs is time- and cost-consuming. The second strategy is to encapsulate 5-azacytidine in nanoparticles to protect it from enzymatic deamination. This concept also makes drug uptake independent of transporters by nanoparticle endocytosis into the targeted cells.<sup>16</sup> Nanoparticulate carriers are introduced for passive drug targeting to tumor tissues through the enhanced permeability and retention (EPR) effect.<sup>17-19</sup> EPR implies that nanoparticles tend to accumulate in tumor tissue much more than they do in normal tissue. However, these explored nanoparticulate delivery systems demonstrate their own disadvantages. Commonly reported drawbacks of colloidal carriers such as liposomes, nanosponges, microemulsions and nanoemulsions, polymeric nanoparticles, and nanocapsules are burst drug release, physical and chemical instability during storage,<sup>20-23</sup> difficulty in industrial fabrication, the presence of organic solvents applied in the production of these systems, some limitations in polymer toxicity<sup>24,25</sup> and many more too

\*Corresponding author: Hamed Hamishehkar, Tel: +98 41 33355965, Fax: +98 41 33346977, Email: Hamishehkarh@tbzmed.ac.ir

©2016 The Authors. This is an Open Access article distributed under the terms of the Creative Commons Attribution (CC BY), which permits unrestricted use, distribution, and reproduction in any medium, as long as the original authors and source are cited. No permission is required from the authors or the publishers.

numerous to mention. All of these disadvantages suggest that these colloidal drug delivery systems are not perfect.<sup>24</sup> Solid lipid nanoparticles (SLNs) were developed in the beginning of the 1990s as drug carriers<sup>26</sup> proposing the superiorities of emulsions, liposomes, and polymeric nanoparticles. The solid lipid matrix is able to protect encapsulated drugs from chemical instability and offer sustaining drug release patterns compared with nanoemulsions.<sup>27,28</sup> SLNs give stable nanosuspension for an extended period of time in comparison with liposomes.<sup>29,30</sup> Furthermore, the SLNs are made of physiologically well-tolerated and generally recognized as safe (GRAS) excipients which reduce the cytotoxicity, leading to their wide variety of applications including dermal, oral, pulmonary, and intravenous use compared with polymeric nanoparticles.<sup>26,31</sup> The greatest benefit of SLNs is the possibility of their industrial scale production.<sup>32-34</sup>

The present study aimed to formulate 5-azacytidine-loaded SLNs for the first time to a) overcome 5-azacytidine instability, and b) increase its anti-tumor performance. The stability of 5-azacytidine was studied via high performance liquid chromatography (HPLC). The cytotoxicity and uptake of the nanoparticulate system were investigated through MTT assay, DAPI staining, Rhodamine B labeling, and Real Time Quantitative Reverse Transcription PCR investigation on the expression of the retinoic acid receptor  $\beta$ 2 (RAR $\beta$ 2) gene of MCF-7 (human breast adenocarcinoma cell line).

## Materials and Methods

### Materials

MCF-7 cell line were purchased from National Cell Bank of Iran (NCBI, Tehran, Iran) 5-azacytidine, fetal bovine serum (FBS), RPMI-1640, DAPI powder, soy

lecithin, Poloxamer® 407 and MTT powder were obtained from Sigma-Aldrich co. Rhodamine B, stearic acid purchased from Merck (Darmstadt, Germany). RNX-plus solution purchased from CinnaGene (CinnaGene, Tehran, Iran), cDNA synthetase kit and SYBR® Premix Ex Taq™II purchased from Takara (Takara, Japan). All other chemicals were of analytical grade. All solutions were prepared with deionized water.

### Methods

#### Preparation of SLN

5-azacytidine (5mg) was dissolved in aqueous solution. Stearic acid and soy lecithin were melted together at 70°C. Stearic acid, a saturated monoacid triglyceride was selected as a negatively charged solid lipid and soy lecithin as a negatively charged low HLB surfactant to increase the chance of positively charged drug encapsulation. The aqueous phase (5 mL) was warmed up to 70°C and added to lipid phase under homogenization (DIAX 900, Heidolph, Germany) at 20000 rpm to form initial w/o emulsion. Then the external water phase and co-surfactant (1% Poloxamer) was added to the initial w/o emulsion under high shear homogenization to form w/o/w emulsion. SLN was finally prepared by cooling down the solution and conversion of emulsion to dispersion by lipid solidification. Since the lipid and surfactant amounts play the major role in size and drug loading capacity of SLNs,<sup>34,35</sup> various formulations were prepared according to change in Stearic acid and soy lecithin (Table 1) and evaluated in the points of size and drug entrapment efficiency. Blank SLN formulation was similarly prepared except that 5-azacytidine was omitted. To prepare fluorescent-labeled SLN, Rhodamine B was used in place of 5-azacytidine.

**Table 1.** Formulation details and characterization results of solid lipid nanoparticles. Data was presented as mean  $\pm$  standard deviation (n=at least 3).

| Code | Stearic acid (mg) | Soy lecithin (mg) | EE <sup>a</sup> (%) | LC <sup>b</sup> (%) | Size (nm)       | PDI <sup>c</sup> | Zeta potential (mv) |
|------|-------------------|-------------------|---------------------|---------------------|-----------------|------------------|---------------------|
| F1   | 20                | 5                 | 18.74 $\pm$ 0.21    | 3.75 $\pm$ 0.04     | 96 $\pm$ 9.34   | 0.31 $\pm$ 0.03  | -18.2 $\pm$ 0.39    |
| F2   | 20                | 10                | 23.14 $\pm$ 0.81    | 3.86 $\pm$ 0.13     | 115 $\pm$ 8.14  | 0.28 $\pm$ 0.01  | -18.7 $\pm$ 0.72    |
| F3   | 20                | 15                | 22.51 $\pm$ 0.32    | 3.22 $\pm$ 0.04     | 186 $\pm$ 7.21  | 0.24 $\pm$ 0.06  | -17.8 $\pm$ 0.23    |
| F4   | 30                | 5                 | 47.34 $\pm$ 0.11    | 6.76 $\pm$ 0.01     | 367 $\pm$ 6.45  | 0.18 $\pm$ 0.02  | -16.3 $\pm$ 0.21    |
| F5   | 30                | 10                | 55.84 $\pm$ 0.46    | 6.98 $\pm$ 0.05     | 204 $\pm$ 10.45 | 0.19 $\pm$ 0.04  | -18.4 $\pm$ 0.34    |
| F6   | 30                | 15                | 45.57 $\pm$ 0.62    | 5.06 $\pm$ 0.07     | 202 $\pm$ 11.34 | 0.25 $\pm$ 0.02  | -16.2 $\pm$ 0.43    |

<sup>a</sup> Encapsulation Efficiency

<sup>b</sup> Loading Capacity

<sup>c</sup> Polydispersity Index

#### Characterization of 5-azacytidine-loaded SLNs

Particles size, size distribution (polydispersity index (PDI)), and zeta potential value of formulations were measured by photon correlation spectroscopy (Nano ZS, Malvern Instruments, UK). For this determination SLN samples were diluted with phosphate buffer saline until appropriate concentration and analyzed in triplicate. Particles Morphology was investigated with scanning electron microscopy (SEM, VEGA TESCAN, Czech Republic). For this analysis, SLN formulations were diluted in de-ionized water and few drops of this diluted SLN suspension were mounted on a glass lamella, air-

dried and gold coated under vacuum. The SEM experiment was carried out on the optimized formulation (F5).

The encapsulation efficiency percent (EE%) and loading capacity percent (LC%) were expressed as the percentage of entrapped 5-azacytidine to the added 5-azacytidine or to the used lipid, respectively. EE was measured by first separation of the un-entrapped 5-azacytidine by centrifugation method using of Amicon® Ultra-15 with molecular weight cutoff of 100 kDa (Millipore, Darmstadt, Germany) tube. The formulation was added to the upper chamber of the Amicon® tube and

then the tube was centrifuged (Sigma 3K30, Darmstadt, Germany) at 5000 rpm for 5 min. The filtrated solution was analyzed by HPLC method under the following conditions: column 150×4.6 mm; ODS-3 5µm, room temperature, acetonitrile/water 40/60 as mobile phase, flow rate 1 ml/min, UV detection at 243 nm, and 20 µl injection volume.<sup>36</sup> The 5-azacytidine EE and LC values were calculated according to the following equations:

$$EE (\%) = \frac{W_{(\text{Initial 5-azacytidine})} - W_{(\text{Free 5-azacytidine})}}{W_{(\text{Initial 5-azacytidine})}} \times 100$$

$$LC (\%) = \frac{W_{(\text{Entrapped 5-azacytidine})}}{W_{(\text{Total lipid})}} \times 100$$

#### *In-vitro release studies*

Drug-loaded SLNs equal to 5 mg of 5-azacytidine was diluted in 5 ml of phosphate buffer (10 mM) pH 7.4, entered into dialysis bag (molecular cut-off of 12,000 Da; Sigma, Steinem, Germany) and immersed into 100 mL phosphate buffer pH 7.4 and 37±0.5°C under stirring. One milliliter of medium during the intervals 1, 2, 4, 6, 8, 12, 24 h was withdrawn and replaced with buffer. To analyze the release kinetics of 5-azacytidine from SLNs, the data of release were subjected to the following equations:

Zero order equation:  $Q_t = K_0 \cdot t$  where  $Q_t$  is the percentage of drug released at time  $t$  and  $k_0$  is the release rate constant; First order equation:  $\ln(100 - Q_t) = \ln 100 - k_1 \cdot t$  where  $k_1$  is the release rate constant; Higuchi's equation:  $Q_t = K_H \cdot t^{1/2}$  where  $k_H$  is the Higuchi release rate constant; Hixson-Crowell:  $(100 - Q_t)^{1/3} = 100^{1/3} - k_{Hc} \cdot t$  where  $k_{Hc}$  is the Hixson-Crowell rate constant. These samples were analyzed by HPLC method as described above.

#### *Cell culture*

the human MCF-7 (human breast adenocarcinoma cell line) were maintained in RPMI-1640 complete growth medium supplemented with 10% FBS, 1% glutamine (2 mM), 1% antibiotic-antimycotic mixture (10000 U/ml penicillin, 10000 mg/ml streptomycin) and bicarbonate sodium 2%. In a humidified incubator (Thermo Fisher Scientific) at 37°C under 5% CO<sub>2</sub> atmosphere. Cells were sub cultured every 2-4 days using Trypsin.

#### *MTT Assay*

To compare effect of encapsulated 5-azacytidine in SLNs with free form of drug and blank SLNs on viability of MCF-7 cell line, we performed MTT assay. Briefly, the MCF-7 cell was seeded in 96-well flat bottom plates. When the cells reached to 40-50% confluence, culture medium were replaced by fresh culture medium containing a range of sample concentration, after 24, 48 h of incubation in a humidified incubator (5% CO<sub>2</sub>) at 37°C, the culture medium were removed carefully from each well, and wells were washed with 200 µl of phosphate buffer saline PBS. The 200 µl fresh culture medium containing 0.5 mg/ml MTT reagent was added

to each well. After 4 h incubation at 37°C, cell culture media was replaced with 200 µl of DMSO and 25 µl of Sorenson buffer (0.1 M glycine, 0.1 M NaCl, pH 10.5). After 30 min of incubation at 37°C in shaking incubator, absorbance was measured at 570 nm using a spectrophotometric plate reader (stat fax@-2100, awareness technology). Cell viability was calculated as the percentage of absorbance in wells with the treated cells versus the control cells.

#### *DAPI Staining Assay*

For analyzing apoptosis in the MCF-7 cell line which is treated with free form of 5-azacytidin and encapsulated 5-azacytidin in SLNs, DAPI staining assay was performed. Briefly, MCF-7 and cell line were seeded in six-well culture plates (100000 cells/well) containing 12 mm sterile cover-slips which is treated with collagen I, after 24 h of incubation in humidified incubator (5% CO<sub>2</sub>) at 37°C, culture medium were replaced with fresh culture medium containing a range of sample concentrations, and with DMSO as positive control for 48 h. then cells were fixed by 4% paraformaldehyde, and permeablized with 0.1% (w/v) Triton X-100 for 5 min, washed in PBS and stained with DAPI work solution and washed again with PBS. Fluorescence Images were obtained with Olympus BX50 microscope, selected wavelengths were 365–375 nm (DAPI, blue).

#### *Rhodamine B uptake studies*

Rhodamine B was used as a fluorescence probe to analyzing the cellular uptake of Rhodamine B loaded SLNs. After encapsulation of Rhodamine B in SLNs unencapsulated Rhodamine B was removed by centrifugal filter devices (Amicon® ultra, ultra cell-50k, Darmstadt, Germany). MCF-7 cell was seeded in six-well culture plates (100000 cells/well), which each well contain 12 mm sterile cover-slip that treated previously with collagen I. seeded cells were incubated in 37°C, 5% CO<sub>2</sub> at humidified incubator for overnight. Then cells were treated with 1 ml of Rhodamine B loaded SLNs and incubated for 2 h and after that period the culture medium was removed and each well washed with PBS, then cells were fixed by 4% paraformaldehyde, and permeablized with 0.1% (w/v) Triton X-100 for 5 min, washed in PBS and stained with DAPI work solution and washed again with PBS. Fluorescence Images were obtained with Olympus BX50 microscope. Selected wavelengths were 365–375 nm (DAPI, blue), 530–550 nm (Rhodamine B, red).

#### *Real-time RT-PCR*

For Real-time RT-PCR analysis, MCF-7 cells (1×10<sup>6</sup>) were plated in 100 mm tissue culture dishes after plating for 24 h, cells were treated with 1µM of free 5-azacytidine and encapsulated 5-azacytidine in SLN for duration of 72 h, Total RNA was extracted from cultured cells with RNX Plus kit as described in the manufactory's manual. RNA concentration and purity were evaluated by agarose gel electrophoresis and

determined by measurement of the absorbance at 260 nm and 280 nm with NanoDrop™ 1000 Spectrophotometer (Thermo Scientific). RNA samples were used as substrate for reverse transcription using a cDNA synthesis kit according to the manufactory's manual. The cDNA was diluted 1:10, and 2 µl were used for each reaction. Real-time PCR was performed with SYBR® Premix Ex Taq™II kit in the Real-time Detection System (Rotor-Gene 6000, Germany). Results were normalized for expression of the housekeeping gene which is GAPDH. For Real-time PCR analysis, primers for qPCR were designed using primer 3.0 web based software with an optimal annealing temperature of 61°C. The sequences of primers for RARβ2 is (sense, 5-GACTGTATGGATGTTCTGTGTCAG-3; antisense, 5-ATTTGTCCTGGCAGACGAAGCA-3), for GAPDH is (sense, 5-ACTTTGGTATCGTGGGAAGGACTC-3; antisense, 5-CAGGGATGATGTTCTGGAGAGC-3). Gene expression was normalized relative to GAPDH using Delta-Delta CT. Experiments were performed in triplicates.

### Statistical Analysis

The experiments were repeated at least in triplicate and data was expressed as the mean ± standard deviation. Statistical analysis was performed using a one-way analysis of variance (one-way ANOVA) with multiple comparisons between deposition data using a Tukey honest significant difference test (SPSS, version 17, Chicago, IL, USA). A P value of <0.05 was considered significant.

## Results and Discussion

### SLN preparation

Particle size is one the most important characteristics of SLNs for successful passive targeting and cellular endocytosis.<sup>37</sup> Average particle sizes of 5-azacytidin-loaded SLNs in different formulations are shown in Table 1.

As can be seen, they ranged from  $96 \pm 9.3$  to  $367 \pm 6.4$  nm. It was claimed that the appropriate size range for the effective cytotoxic performance of nanoparticles is <200 nm.<sup>16</sup> Therefore, most formulations in this study were in the suitable size range. The PDI of SLNs was found to be in the range of 0.18 to 0.31 (Table 1). The narrow size distribution of the carriers guarantees uniform drug delivery to the target tissue. A PDI below 0.2 is considered as a uniform size distribution.<sup>38</sup> The PDI of formulations F4 and F5 were 0.18 and 0.19, respectively. The SEM image which supports the size data is shown in Figure 1.

Zeta potential is another key parameter for the colloidal stability of nanoparticles. It has been reported that zeta potential values  $\pm 30$  mV are considered suitable and effective for the colloidal stability of nanosuspensions. The zeta potential of all formulations was almost in the same range (-16.2 to -18.7 mV) as shown in Table 1. Although the zeta potential of formulation were in the lower range, an appropriate size stability was found after

6 months (data not shown), probably because of the hindering effect of the polymeric co-surfactant (poloxamer) used in the external aqueous phase to stabilize nanoparticles.<sup>39</sup> 5-azacytidine is a hydrophilic material; therefore, it can be predicted that its effective encapsulation into lipid-based nanocarriers would be problematic. Hopefully, by using the double emulsion technique and an adequate amount of inner phase surfactant, the appropriate percent of drug entrapment can be achieved (Table 1). Furthermore, negative charge lipid (stearic acid) may be helpful in the appropriate encapsulation of a positively-charged drug. In this study, the percentages of EE and LC were 18.7 to 55.8 and 3.2 to 7.0, respectively. Because of the highest LC and zeta potential values, the almost lowest PDI value, and the appropriate size, the F5 formulation was selected as the optimized one used for in vitro cytotoxic investigations (MTT assay, Real time RT-PCR, Rhodamine B uptake and DAPI staining).

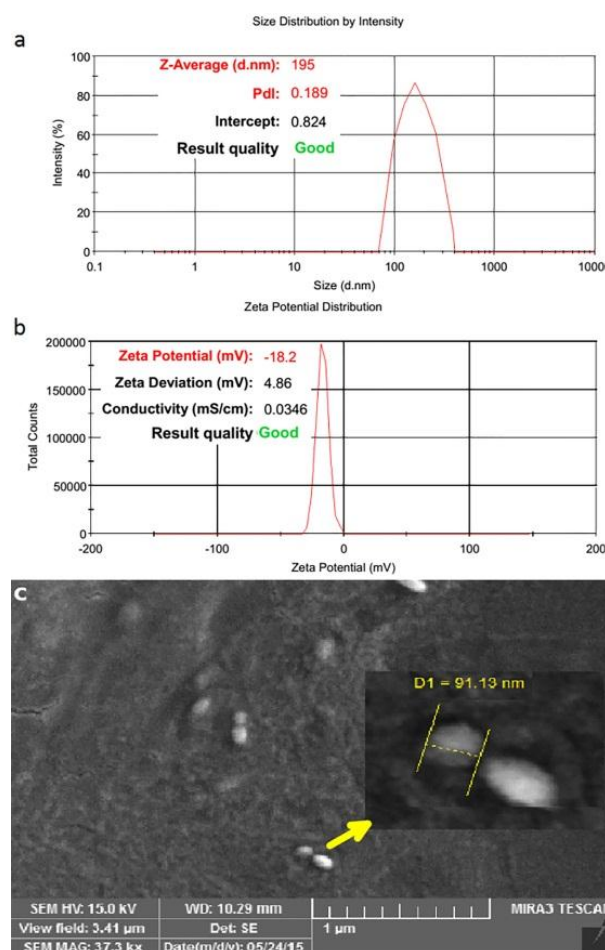


**Figure 1.** Size (a), zeta potential (b), and scanning electron microscopy images (c) of optimized 5-azacytidin-loaded solid lipid nanoparticles.

### In vitro drug release study

The formulations prepared with high surfactant amounts (F3 and F5) presented faster drug release (Figure 2) than the others.



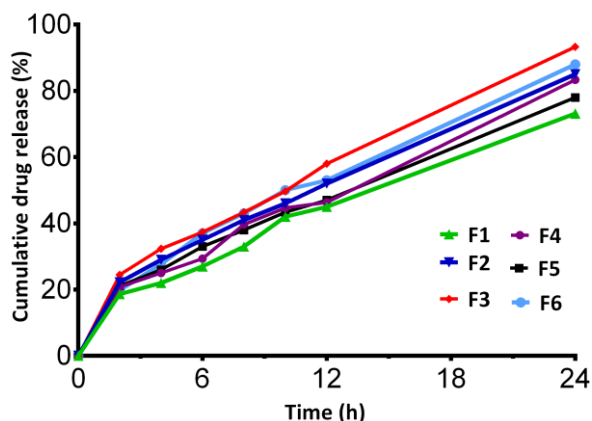


**Figure 2.** *In vitro* drug release profile for different formulations of 5-azacytidine-loaded solid lipid nanoparticles.

The presence of lipophilic surfactant in the lipid matrix structure might have enhanced water penetration into the matrix via emerged pores and caused drug leakage and release in higher values than the others. The SLNs fabricated with a higher lipid amount released drug in a slower pattern as well. All formulations released more than 80% of drug during 24 h, indicating potentially

enough release of drug in targeted cancer tissue after formulation administration. Therefore, there was an initial 20% burst release, and the remaining 60% released during 24 h, which may be a suitable drug release pattern for efficient drug accumulation in cancer cells.<sup>40</sup> To define the kinetics of 5-azacytidine release from controlled release drug carriers, different mathematical models have been suggested. The zero order model defines drug delivery systems where the release of drug is not dependent on its concentration.<sup>41</sup> The formulators prefer to develop drug delivery systems which release drug in a zero order manner to achieve a steady release of drug.<sup>42</sup> The first order kinetic explains release from carriers where the release rate is concentration-dependent.<sup>41</sup> Drug release in the Higuchi model is directly related to a square root of time based on the Fickian diffusion.<sup>43</sup> The Hixson-Crowell cube root equation explains the changes of drug release by change in surface area and diameter of the particles with time and is mostly used in the case of drug carriers which dissolve or erode over time.<sup>44</sup> The *in vitro* drug release indicated that all formulations resulted in zero order drug release kinetics (Table 2).

**Table 2.** Kinetic parameters of 5-azacytidine release from the solid lipid nanoparticles

|    | Zero-order                |                | First-order              |                | Higuchi                     |                | Hixson-Crowell            |                |
|----|---------------------------|----------------|--------------------------|----------------|-----------------------------|----------------|---------------------------|----------------|
|    | $K_0$ (%h <sup>-1</sup> ) | R <sup>2</sup> | $K_1$ (h <sup>-1</sup> ) | R <sup>2</sup> | $K_H$ (%h <sup>-1/2</sup> ) | R <sup>2</sup> | $K_0$ (%h <sup>-1</sup> ) | R <sup>2</sup> |
| F1 | 0.025                     | 0.991          | 0.052                    | 0.985          | 0.162                       | 0.970          | 0.013                     | 0.993          |
| F2 | 0.028                     | 0.999          | 0.075                    | 0.963          | 0.180                       | 0.974          | 0.018                     | 0.984          |
| F3 | 0.031                     | 0.998          | 0.111                    | 0.934          | 0.198                       | 0.969          | 0.023                     | 0.969          |
| F4 | 0.029                     | 0.992          | 0.072                    | 0.954          | 0.182                       | 0.955          | 0.017                     | 0.975          |
| F5 | 0.028                     | 0.998          | 0.058                    | 0.975          | 0.164                       | 0.973          | 0.015                     | 0.989          |
| F6 | 0.030                     | 0.990          | 0.086                    | 0.964          | 0.195                       | 0.987          | 0.020                     | 0.987          |

**MTT assay study**

MTT assay has been widely used to measure cell viability. Figure 3 shows the percentage of MCF-7 cell survival after exposure to blank SLN and 5-azacytidine, either free or loaded in SLNs.

Encapsulated drug shows a higher cytotoxicity for MCF-7 in 48 hours of treatment than in 24 hours. This result may have been caused by different parameters such as drug release, drug degradation rate, and the doubling time of the MCF-7 cell line which is approximately 24-48 hours.<sup>45</sup> 5-azacytidine inhibits DNA methyltransferases<sup>46</sup> (the enzymes responsible for *de novo* methylation of the new synthesized DNA during the S-phase and the maintenance of methylation).<sup>7</sup> Therefore, prolonged exposure of cancer cells to this drug is essential for optimal efficacy. It has been reported that the elimination half-life of 5-azacytidine is about 4 hours (i.v. or s.c. administration).<sup>47</sup> Therefore, drug encapsulation in SLNs might increase its stability. This may explain the superiority of drug-loaded SLNs cytotoxicity performance to free drug in 48 h incubation.

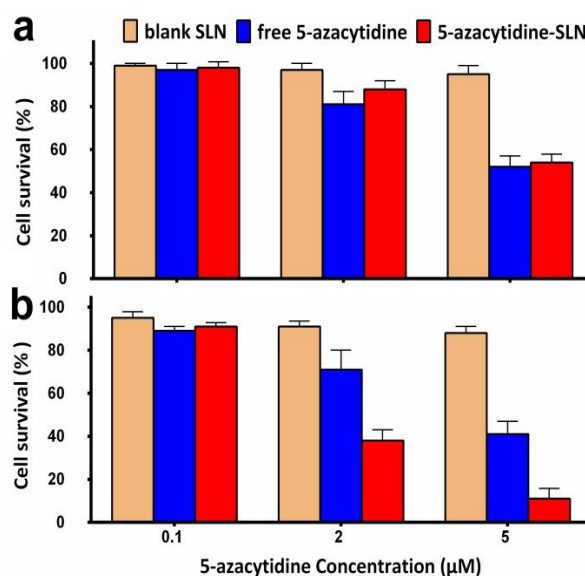


**Figure 3.** Dose dependent study of MCF-7 (breast cancer cell line) survival in exposure to free 5-azacytidine, encapsulated 5-azacytidin and blank solid lipid nanoparticles (SLN) in 24h (a) and 48h (b). Data is presented as mean ± standard deviation (n=6).

**DAPI staining**

To observe the different effects of free 5-azacytidine and loaded 5-azacytidine on the morphology of cell nuclei, DAPI staining was performed. DAPI was used for visualizing apoptotic cells for which nuclear DNA fragmentation and condensed chromosome were considered.<sup>48</sup> Figure 4 shows the images of untreated control cells and treated MCF-7 cells which were stained with DAPI after exposure to free 5-azacytidine and loaded 5-azacytidine in SLNs for about 48 hours. The morphological changes of the nuclear chromatin in both cells treated with free 5-azacytidine and encapsulated 5-azacytidine indicate programmed cell death (apoptosis).

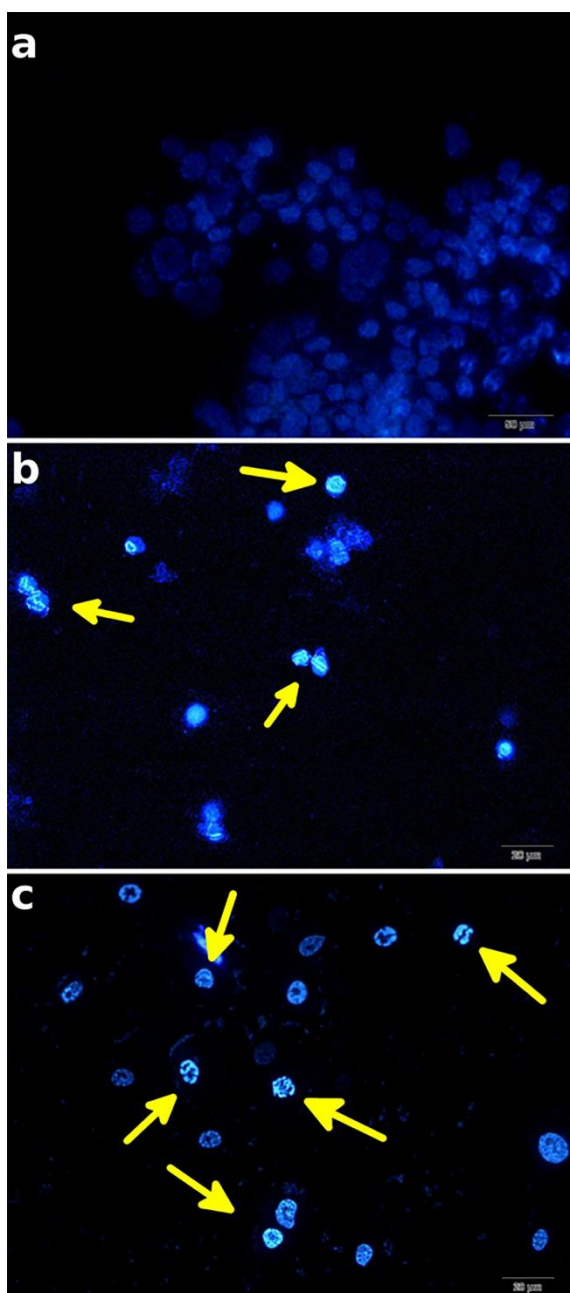


**Figure 4.** Fluorescent images of DAPI staining of untreated MCF-7 (a), and those treated with 5-azacytidine solution (5  $\mu$ M) (b) and 5-azacytidine-loaded solid lipid nanoparticles in equivalent concentration (c).

**Relative uptake of SLNs in MCF-7**

To confirm the uptake of SLNs into MCF-7 cells, Rhodamine B-loaded SLNs were used to incubate cultured cell lines within 2 h and were analyzed by fluorescent microscope. Free form Rhodamine B and blank SLN were used as negative controls to eliminate any interference which is negligible fluorescence. As shown in Figure 5, Rhodamine B is red and the cell nucleus stained with DAPI is blue. After 2 h of incubation, a bright light appeared within the cells indicating that SLNs particles were internalized into the cells. The pictures of cells show a comparable difference among MCF-7 cells after 5 minutes and after 2 hours. The study of Rhodamine b-loaded blank SLNs clearly show the time-dependent increase in fluorescence intensity inside the MCF-7 which was caused by the uptake of Rhodamine B-loaded SLNs. SLNs accumulated in the cytoplasm after uptake by MCF-7 cells.

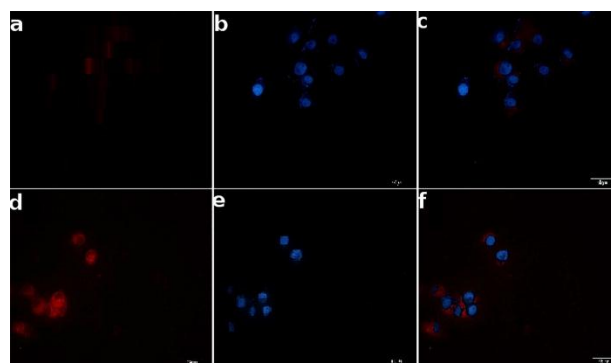


**Figure 5.** Fluorescence images of the cells incubated with the Rhodamine B labeled solid lipid nanoparticles (SLNs) for 5 min (a) and 2h (d) and after those visualized with DAPI (b and e). The merged Figures were used to show the cell localization of SLNs (c and f).

**Real time RT-PCR**

Epigenetic modification plays a crucial role on gene expression. Cancer cells use epigenetic modifications for silencing tumor suppressors. Breast cancer is greatly modified by epigenetic mechanisms, mostly the hypermethylation of CpG islands.<sup>49</sup> Aberrant methylation of the retinoic acid receptor  $\beta$ 2 (RAR $\beta$ 2) promotor was reported in the MCF-7 cell line,<sup>50</sup> which is responsible for the low expression of the RAR $\beta$ 2 gene. In the current study, RAR $\beta$ 2 gene expression was measured after treatment with encapsulated 5-azacytidine and free 5-azacytidine with Real Time qRT-PCR. Figure 6 shows the expression of RAR $\beta$ 2 mRNA for treated cells with 1  $\mu$ M free 5-azacytidine and encapsulated. The current study showed no significant difference ( $p > 0.05$ ) between free form and encapsulated 5-azacytidine. This result shows that the drug was still effective after the encapsulation procedure.

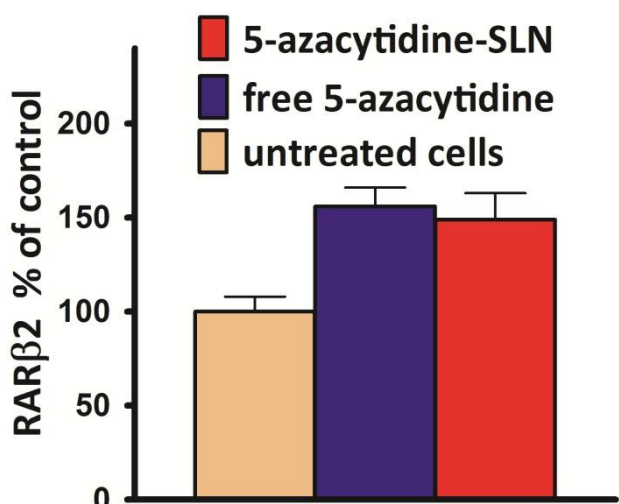


**Figure 6.** Expression of retinoic acid receptor  $\beta 2$  (RAR $\beta 2$ ) gene after 3 days treatment of MCF-7 cells with 1  $\mu$ M free 5-azacytidine and equivalent concentration of 5-azacytidine-loaded solid lipid nanoparticles (SLN). Glyceraldehyde 3-phosphate dehydrogenase (GAPDH) was used as an internal control. Data were expressed as means  $\pm$  standard deviation.

### Conclusion

The developed SLN showed promising 5-azacytidine encapsulation probably due to the ion-pair interaction of the negatively charged lipid with the positively charged drug. *In vitro* cell cytotoxicity experiments proved the better performance of 5-azacytidine-loaded SLN than free 5-azacytidine, which may be attributed to better endocytosis of nanoparticulate carriers and higher drug stability. Real Time qRT-PCR confirmed that 5-azacytidine remained stable during SLN preparation and encapsulation by almost the same performance in gene expression. The poor loading capacity, however, is a major disadvantage of SLN formulation. The results of this study pave the way for introducing an efficient formulation of 5-azacytidine for cancer therapy.

### Acknowledgments

The authors would like to thank the drug applied research center, Tabriz University of Medical Sciences for financial support (93/310). This article is part of an MSc thesis (93/2-7/9) of clinical biochemistry submitted in Faculty of Medicine, Tabriz University of Medical Sciences.

### Ethical Issues

Not applicable.

### Conflict of Interest

The authors report no conflicts of interest.

### References

- Piskala A, Šorm F. Nucleic acids components and their analogues. LI. Synthesis of 1-glycosyl derivatives of 5-azauracil and 5-azacytosine. *Collect Czech Chem Commun* 1964;29(9):2060-76. doi: 10.1135/cccc19642060
- Li LH, Olin EJ, Buskirk HH, Reineke LM. Cytotoxicity and mode of action of 5-azacytidine on I1210 leukemia. *Cancer Res* 1970;30(11):2760-9.
- Karon M, Sieger L, Leimbrock S, Finklestein JZ, Nesbit ME, Swaney JJ. 5-azacytidine: A new active agent for the treatment of acute leukemia. *Blood* 1973;42(3):359-65.
- Von Hoff DD, Slavik M, Muggia FM. 5-azacytidine. A new anticancer drug with effectiveness in acute myelogenous leukemia. *Ann Intern Med* 1976;85(2):237-45.
- Kaminskas E, Farrell A, Abraham S, Baird A, Hsieh LS, Lee SL, et al. Approval summary: Azacitidine for treatment of myelodysplastic syndrome subtypes. *Clin Cancer Res* 2005;11(10):3604-8. doi: 10.1158/1078-0432.CCR-04-2135
- Vesely J, Čihák A. 5-Azacytidine: mechanism of action and biological effects in mammalian cells. *Pharmacol Therapeut A* 1978;2(4):813-40. doi:10.1016/0362-5478(78)90016-5
- Christman JK. 5-azacytidine and 5-aza-2'-deoxycytidine as inhibitors of DNA methylation: Mechanistic studies and their implications for cancer therapy. *Oncogene* 2002;21(35):5483-95. doi: 10.1038/sj.onc.1205699
- Schaefer M, Hagemann S, Hanna K, Lyko F. Azacytidine inhibits rna methylation at dnmt2 target sites in human cancer cell lines. *Cancer Res* 2009;69(20):8127-32. doi: 10.1158/0008-5472.CAN-09-0458
- David GL, Yegnasubramanian S, Kumar A, Marchi VL, De Marzo AM, Lin X, et al. Mdr1 promoter hypermethylation in mcf-7 human breast cancer cells: Changes in chromatin structure induced by treatment with 5-aza-cytidine. *Cancer Biol Ther* 2004;3(6):540-8.
- Aparicio A, Weber JS. Review of the clinical experience with 5-azacytidine and 5-aza-2'-deoxycytidine in solid tumors. *Curr Opin Investig Drugs* 2002;3(4):627-33.
- Howell PM, Liu Z, Khong HT. Demethylating agents in the treatment of cancer. *Pharmaceut* 2010;3(7):2022-44. doi:10.3390/ph3072022
- Chan KK, Giannini DD, Staroscik JA, Sadee W. 5-azacytidine hydrolysis kinetics measured by high-pressure liquid chromatography and <sup>13</sup>c-nmr spectroscopy. *J Pharm Sci* 1979;68(7):807-12.
- Mahfouz RZ, Jankowska A, Ebrahim Q, Gu X, Visconte V, Tabarroki A, et al. Increased cda expression/activity in males contributes to decreased cytidine analog half-life and likely contributes to worse outcomes with 5-azacytidine or decitabine therapy. *Clin Cancer Res* 2013;19(4):938-48. doi: 10.1158/1078-0432.CCR-12-1722
- Rius M, Stresemann C, Keller D, Brom M, Schirmacher E, Keppler D, et al. Human concentrative nucleoside transporter 1-mediated uptake of 5-azacytidine enhances DNA

- demethylation. *Mol Cancer Ther* 2009;8(1):225-31. doi: 10.1158/1535-7163.MCT-08-0743
15. Brueckner B, Rius M, Markelova MR, Fichtner I, Hals PA, Sandvold ML, et al. Delivery of 5-azacytidine to human cancer cells by elaidic acid esterification increases therapeutic drug efficacy. *Mol Cancer Ther* 2010;9(5):1256-64. doi: 10.1158/1535-7163.MCT-09-1202
  16. Martins S, Costa-Lima S, Carneiro T, Cordeiro-da-Silva A, Souto EB, Ferreira DC. Solid lipid nanoparticles as intracellular drug transporters: An investigation of the uptake mechanism and pathway. *Int J Pharm* 2012;430(1-2):216-27. doi: 10.1016/j.ijpharm.2012.03.032
  17. Danhier F, Feron O, Preat V. To exploit the tumor microenvironment: Passive and active tumor targeting of nanocarriers for anti-cancer drug delivery. *J Control Release* 2010;148(2):135-46. doi: 10.1016/j.jconrel.2010.08.027
  18. Salehi R, Rasouli S, Hamishehkar H. Smart thermo/pH responsive magnetic nanogels for the simultaneous delivery of doxorubicin and methotrexate. *Int J Pharm* 2015;487(1-2):274-84. doi: 10.1016/j.ijpharm.2015.04.051
  19. Salehi R, Hamishehkar H, Eskandani M, Mahkam M, Davaran S. Development of dual responsive nanocomposite for simultaneous delivery of anticancer drugs. *J Drug Target* 2014;22(4):327-42. doi: 10.3109/1061186X.2013.876645
  20. Hamishehkar H, Rahimpour Y, Kouhsoltani M. Niosomes as a propitious carrier for topical drug delivery. *Expert Opin Drug Deliv* 2013;10(2):261-72. doi: 10.1517/17425247.2013.746310
  21. Rahimpour Y, Hamishehkar H. Liposomes in cosmeceutics. *Expert Opin Drug Deliv* 2012;9(4):443-55. doi: 10.1517/17425247.2012.666968
  22. Ghaderi S, Ghanbarzadeh S, Mohammadhassani Z, Hamishehkar H. Formulation of gammaoryzanol-loaded nanoparticles for potential application in fortifying food products. *Adv Pharm Bull* 2014;4(Suppl 2):549-54. doi: 10.5681/apb.2014.081
  23. Mahdavi H, Mirzadeh H, Hamishehkar H, Jamshidi A, Fakhari A, Emami J, et al. The effect of process parameters on the size and morphology of poly(D, L-Lactide-Co-Glycolide) micro/nanoparticles prepared by an oil in oil emulsion/solvent evaporation technique. *J Appl Polym Sci* 2010;116(1):528-34. doi: 10.1002/app.31595
  24. Selvamuthukumar S, Velmurugan R. Nanostructured lipid carriers: A potential drug carrier for cancer chemotherapy. *Lipids Health Dis* 2012;11:159. doi: 10.1186/1476-511X-11-159
  25. Smith A. Evaluation of poly (lactic acid) as a biodegradable drug delivery system for parenteral administration. *Int J Pharm* 1986;30(2-3):215-20. doi:10.1016/0378-5173(86)90081-5
  26. Muller RH, Mader K, Gohla S. Solid lipid nanoparticles (sln) for controlled drug delivery - a review of the state of the art. *Eur J Pharm Biopharm* 2000;50(1):161-77.
  27. Ezzati Nazhad Dolatabadi J, Valizadeh H, Hamishehkar H. Solid lipid nanoparticles as efficient drug and gene delivery systems: Recent breakthroughs. *Adv Pharm Bull* 2015;5(2):151-9. doi: 10.15171/apb.2015.022
  28. Ghanbarzadeh S, Hariri R, Kouhsoltani M, Shokri J, Javadzadeh Y, Hamishehkar H. Enhanced stability and dermal delivery of hydroquinone using solid lipid nanoparticles. *Colloids Surf B Biointerfaces* 2015;136:1004-10. doi: 10.1016/j.colsurfb.2015.10.041
  29. Souto EB, Wissing SA, Barbosa CM, Muller RH. Development of a controlled release formulation based on sln and nlc for topical clotrimazole delivery. *Int J Pharm* 2004;278(1):71-7. doi: 10.1016/j.ijpharm.2004.02.032
  30. Ezzati Nazhad Dolatabadi J, Hamishehkar H, Eskandani M, Valizadeh H. Formulation, characterization and cytotoxicity studies of alendronate sodium-loaded solid lipid nanoparticles. *Colloids Surf B Biointerfaces* 2014;117:21-8. doi: 10.1016/j.colsurfb.2014.01.055
  31. Hamishehkar H, Shokri J, Fallahi S, Jahangiri A, Ghanbarzadeh S, Kouhsoltani M. Histopathological evaluation of caffeine-loaded solid lipid nanoparticles in efficient treatment of cellulite. *Drug Dev Ind Pharm* 2015;41(10):1640-6. doi: 10.3109/03639045.2014.980426
  32. Müller R, Lippacher A, Gohla S. Solid lipid nanoparticles (SLN) as a carrier system for the controlled release of drugs. USA: Marcel Dekker; 2000.
  33. Bhaskar K, Anbu J, Ravichandiran V, Venkateswarlu V, Rao YM. Lipid nanoparticles for transdermal delivery of flurbiprofen: Formulation, in vitro, ex vivo and in vivo studies. *Lipids Health Dis* 2009;8:6. doi: 10.1186/1476-511X-8-6
  34. Severino P, Andreani T, Macedo AS, Fanguero JF, Santana MH, Silva AM, et al. Current state-of-art and new trends on lipid nanoparticles (sln and nlc) for oral drug delivery. *J Drug Deliv* 2012;2012:750891. doi: 10.1155/2012/750891
  35. Schmidts T, Dobler D, Nissing C, Runkel F. Influence of hydrophilic surfactants on the properties of multiple w/o/w emulsions. *J Colloid Interface Sci* 2009;338(1):184-92. doi: 10.1016/j.jcis.2009.06.033
  36. Galloni C, Azzarà VG, Loardi G. TCH-016 Extended Chemical-Physical Stability of 25 mg/ml Azacitidine Suspension. *Eur J Hosp Pharm Sci Pract* 2013;20(Suppl 1):A74-A. doi:10.1136/ejpharm-2013-000276.207
  37. Murugan K, Choonara YE, Kumar P, Bijukumar D, du Toit LC, Pillay V. Parameters and characteristics governing cellular internalization and trans-barrier trafficking of nanostructures. *Int J Nanomedicine* 2015;10:2191-206. doi: 10.2147/IJN.S75615



38. Das S, Ng WK, Tan RB. Are nanostructured lipid carriers (nlcs) better than solid lipid nanoparticles (slns): Development, characterizations and comparative evaluations of clotrimazole-loaded slns and nlcs? *Eur J Pharm Sci* 2012;47(1):139-51. doi: 10.1016/j.ejps.2012.05.010
39. Heurtault B, Saulnier P, Pech B, Proust JE, Benoit JP. Physico-chemical stability of colloidal lipid particles. *Biomaterials* 2003;24(23):4283-300.
40. Allen TM, Cullis PR. Drug delivery systems: Entering the mainstream. *Science* 2004;303(5665):1818-22. doi: 10.1126/science.1095833
41. Desai SJ, Simonelli AP, Higuchi WI. Investigation of factors influencing release of solid drug dispersed in inert matrices. *J Pharm Sci* 1965;54(10):1459-64.
42. Hughes GA. Nanostructure-mediated drug delivery. *Nanomedicine* 2005;1(1):22-30. doi: 10.1016/j.nano.2004.11.009
43. Higuchi T. Mechanism of sustained-action medication. Theoretical analysis of rate of release of solid drugs dispersed in solid matrices. *J Pharm Sci* 1963;52:1145-9.
44. Hixson AW, Crowell JH. Dependence of reaction velocity upon surface and agitation. *Ind Eng Chem* 1931;23(10):1160-8. doi: 10.1021/ie50262a025
45. Sutherland RL, Hall RE, Taylor IW. Cell proliferation kinetics of mcf-7 human mammary carcinoma cells in culture and effects of tamoxifen on exponentially growing and plateau-phase cells. *Cancer Res* 1983;43(9):3998-4006.
46. Brueckner B, Garcia Boy R, Siedlecki P, Musch T, Kliem HC, Zielenkiewicz P, et al. Epigenetic reactivation of tumor suppressor genes by a novel small-molecule inhibitor of human DNA methyltransferases. *Cancer Res* 2005;65(14):6305-11. doi: 10.1158/0008-5472.CAN-04-2957
47. Kaminskas E, Farrell AT, Wang YC, Sridhara R, Pazdur R. Fda drug approval summary: Azacitidine (5-azacytidine, vidaza) for injectable suspension. *Oncologist* 2005;10(3):176-82. doi: 10.1634/theoncologist.10-3-176
48. Tone S, Sugimoto K, Tanda K, Suda T, Uehira K, Kanouchi H, et al. Three distinct stages of apoptotic nuclear condensation revealed by time-lapse imaging, biochemical and electron microscopy analysis of cell-free apoptosis. *Exp Cell Res* 2007;313(16):3635-44. doi: 10.1016/j.yexcr.2007.06.018
49. Jovanovic J, Ronneberg JA, Tost J, Kristensen V. The epigenetics of breast cancer. *Mol Oncol* 2010;4(3):242-54. doi: 10.1016/j.molonc.2010.04.002
50. Arapshian A, Kuppumbatti YS, Mira-y-Lopez R. Methylation of conserved cpg sites neighboring the beta retinoic acid response element may mediate retinoic acid receptor beta gene silencing in mcf-7 breast cancer cells. *Oncogene* 2000;19(35):4066-70. doi: 10.1038/sj.onc.1203734